

Differentiation of Benign and Malignant Parotid Gland Tumors with MRI and Diffusion Weighted Imaging

Benign ve Malign Parotid Gland Tümörlerinin Ayrımında Manyetik Rezonans ve Difüzyon Ağırlıklı Görüntüleme

Umut Percem ORHAN SOYLEMEZ[®], Basak ATALAY[®]

Ethics Committee Approval: This study was approved by Istanbul Medeniyet University Göztepe Educational and Research Hospital Ethics Committee, 22 July 2020, 2020/0482.
Conflict of interest: The authors declare that they have no conflict of interest.
Funding: None.
Informed Consent: Informed consents were taken from the participants of the study.

Cite as: Orhan Söylemez UP, Atalay B. Differentiation of benign and malignant parotid gland tumors with MRI and diffusion weighted imaging. Medeni Med J. 2021;36:138-45.

ABSTRACT

Objective: This study investigated the effectivity of Magnetic Resonance Imaging (MRI) findings and Apparent Diffusion Coefficient (ADC) value in evaluating parotid gland tumors (PGTs), and aimed to reduce the biopsy procedure before surgery.

Methods: This retrospective study included 54 PGTs of 42 patients' (24 female, 18 male, mean age; 51.4±15.9). All of the patients had an MRI, and histopathologic diagnosis. The signal intensity [T1 and T2 Weighted (W), T1W after intravenous contrast agent injection] and mean ADC values of the PGTs were measured. Also contrast enhancement pattern (homogenous, heterogeneous, peripheral or none), margin features (well or ill-defined), sizes, location (superficial lobe/deeplobe/both), perineural spread, presence of lymphadenopathy, and extension to adjacent structures were noted.

Results: The distribution of PGTs was; 21 pleomorphic adenomas, 18 Warthin tumors, 2 lymph nodes, 2 mucoepidermoid carcinomas, 5 adenoid cystic carcinoma, 1 basal cell carcinoma, 2 metastases and 2 lymphomas; (13 malignant and 41 benign lesions). Morphologic parameters; ill-defined margin, perineural spread, lymphadenopathy, and extension to adjacent structures were found to be significantly associated with malign lesions ($p<0.01$). There was a significant difference between ADC values of malignant and benign PGTs ($p<0.05$). Also ADC values and T2 signal intensity was significantly lower in Warthin tumors rather than pleomorphic adenomas ($p<0.05$).

Conclusions: Mean ADC values when considered with morphological features may be accessible methods to distinguish benign and malignant PGTs, also ADC values and T2 signal intensity may be useful for differentiating pleomorphic adenomas from Warthin tumors, thereby reducing the number of biopsies and thus complications.

Keywords: Apparent diffusion coefficient, magnetic resonance imaging, neoplasms, parotid gland

ÖZ

Amaç: Bu çalışmada biyopsi işlemlerini azaltmak amacı ile Manyetik Rezonans Görüntülemenin (MRG) parotis gland tümörlerinin (PGT) malign-benign ayrımındaki etkinliği değerlendirilmiştir ve operasyon öncesi biyopsi işleminin azaltılması amaçlanmıştır.

Yöntem: 42 hastaya (24 kadın, 18 erkek, ortalama yaş; 51,4±15,9) ait 54 parotis gland lezyonu çalışmaya dahil edildi. Tüm hastaların MR görüntüleri ve histopatolojik sonuçları retrospektif olarak tarandı. PGT'lerin T1, T2 ağırlıklı sekanslarda ve kontrast verimi sonrasında sinyal intensiteleri ve ortalama ADC değerleri ölçüldü. Diğer yandan lezyonların kontrastlanma paterni (homojen, heterojen, periferik veya kontrastlanmayan), sınırları (iyi veya kötü sınırlı), boyutları, lokalizasyonları (yüzeysel lob/derin lob/ her ikisi), perinöral yayılım, lenfadenopati varlığı ve komşu dokulara ekstansiyon değerlendirildi.

Bulgular: PGT'lerin dağılımı; 13 malign ve 41 benign lezyon olmak üzere 21 pleomorfik adenom, 18 Warthin tümörü, 3 lenf nodu, 2 mucoepidermoid karsinom, 5 adenoid kistik karsinom, 1 bazal hücreli karsinom, 2 metastaz ve 2 lenfoma şeklindedir. Morfolojik parametrelerden kötü sınır, perinöral yayılım, lenfadenopati varlığı ve çevre doku uzanım malign lezyonlarla anlamlı ilişkili bulundu ($p<0.01$). Malign lezyonların ADC değerleri benignlere göre anlamlı olarak düşük bulundu ($p<0.05$). Ayrıca Warthin tümörlerinde ADC değerleri ve T2 sinyal intensitesi, pleomorfik adenomlardan istatistiksel olarak anlamlı şekilde daha düşüktü ($p<0.05$).

Sonuç: Morfolojik özelliklerle birlikte ortalama ADC değerleri malign tümörleri benignlerden, ADC değerleri ve T2 sinyalleri ise pleomorfik adenomları Warthin tümörlerinden ayırmaya yardımcı olarak biyopsi sayılarını dolayısıyla komplikasyonlarını azaltabilir.

Anahtar kelimeler: Görünür difüzyon katsayısı, manyetik rezonans görüntüleme, neoplazm, parotis bezi

Received: 1 February 2021

Accepted: 4 May 2021

Online First: 18 June 2021

Corresponding Author:

B. Atalay

ORCID: 0000-0003-3318-3555

Istanbul Medeniyet University

Faculty of Medicine, Goztepe

Training and Research Hospital,

Department of Radiology,

Istanbul, Turkey

✉ basak_hosgoren@yahoo.com

U.P. Orhan Söylemez

ORCID: 0000-0002-8164-7847

Istanbul Medeniyet University

Faculty of Medicine Goztepe

Training and Research Hospital,

Department of Radiology,

Istanbul, Turkey



INTRODUCTION

Salivary gland tumors constitute 3% of head and neck tumors. Seventy percent of them are located in the parotid gland^{1,2}. They can also be detected in the submandibular gland, small salivary and sublingual glands³. The majority of parotid gland tumors are benign. Pleomorphic adenoma is the most common type of parotid gland tumor and Warthin tumors are the second most common^{4,5}. The most frequent type of malignant parotid tumor is mucoepidermoid carcinoma, which occurs in 15% and 30% of the cases⁶. Apart from differentiating benign and malignant parotid gland tumors (PGTs), it is important to distinguish between pleomorphic adenomas and Warthin tumors. While total radical parotidectomy is the preferred treatment modality in pleomorphic adenomas, conservative approaches may be applied for Warthin tumors. In addition, radiotherapy following total parotidectomy is the mainstream treatment modality for malignant lesions^{4,7}.

A concise diagnosis of these lesions may enable the surgeon to make a diagnosis, and perform the treatment at a single occasion. At that point, Magnetic Resonance Imaging (MRI) can play an important role in providing information about the location, and extension of the lesion, presence of perineural spread, nodal and distant metastases⁴. The advances in diffusion weighted imaging (DWI) play important roles in distinguishing benign and malignant tumors by providing information on the microcirculation and microcellularity of the tumors⁸. To this respect, we hypothesized that signal intensity (SI) and Apparent Diffusion Coefficient (ADC) values can be used to differentiate malignant and benign parotid gland tumors based on differences in cellularity. We aimed to evaluate the diagnostic performance of conventional MRI and DWI in parotid gland tumors.

MATERIAL and METHOD

The institutional Review Board approved this retrospective study (approval no: 2020/0482) in which the images of 64 PGTs of 52 patients obtained at a single center between August 2018 and April 2020. The images were obtained from the hospital's picture archiving and communication system (PACS). The inclusion criteria were as follows: MRI of the face or neck covering the entire parotid gland with an adequate image quality for assessment, having a lesion in the parotid gland, and a histopathologic diagnosis of the fine needle aspiration biopsy (FNAB) or parotidectomy specimens.

The exclusion criteria for both groups were as follows: lack of MRI or MRI with inadequate image quality (motion artifacts or missing evaluation criteria), an MRI diagnosis that was not verified histopathologically, age <18 years, and/or proven inflammatory or vascular lesions.

Magnetic Resonance Imaging

All MRI examinations were performed with a General Electric Signa Excite 1.5 Tesla MRI device. The examination protocol included axial and sagittal T2W (weighted) fast spin echo (FSE) without fat suppression, axial and coronal T1W FSE with fat suppression, and coronal T2W FSE with fat suppression. After the contrast administration, axial and coronal T1W FSE sequences with fat suppression were performed.

The imaging parameters were the following: T1W: (TR/TE 445/11 ms); T2W: (TR/TE 8442/9102 ms); field of view, 22-24 cm; matrix, 256×192; section thickness, 3 mm; section gap, 1.5 mm. DWI was done using an echo-planar single-shot spin-echo sequence in the axial plane (TR/TE 8124/80 ms), with b values of 0 and 1000 s/mm². The ADC maps were generated automatically. After intravenous injection of 0.1 mmol/kg gadopentetic acid, the contrast-enhanced images were obtained.

Measurement Protocol

The data projection images were recorded and reconstructed using the local hospital PACS to measure the determined SI and ADC values. For all lesions, the SI in T1W and T2W images, SI after contrast injection and the mean ADC values were measured. The contrast enhancement patterns (homogenous, heterogeneous, peripheral, or none), borders (well or ill-defined), tumor sizes (<1cm, 1-2 cm, 2-3 cm, >3 cm), involved lobes (superficial, deep, superficial and deep lobe), presence of extension into adjacent structures, perineural spread, and lymphadenopathy were noted. The SI and ADC values were measured with the region of interest (ROI). The ROI was as wide as possible based on the size of the lesion. After measuring the T1, T2, and post-contrast T1 SI, a copy of the same ROI was placed on the ADC maps (Figure 1). The ROI was placed to avoid cystic, necrotic, and hemorrhagic areas. If there was heterogeneity in the SI and ADC appearance, the average of the lowest and highest values was taken.

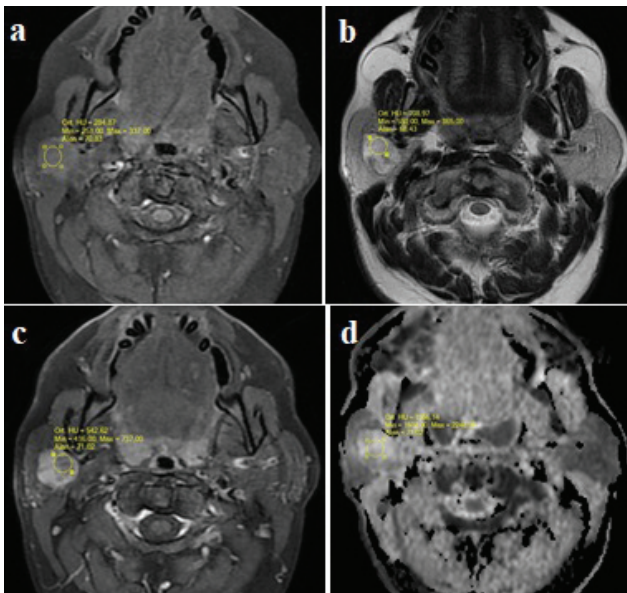


Figure 1. Signal intensity and ADC value measurements of a pleomorphic adenoma (ROIs) 1a: T1W axial image. A slightly hyperintense lesion in the superficial lobe of the right parotid gland 1b: T2W axial image. The lesion is hyperintense with hypointense nodular areas 1c: T1W fat-saturated image with contrast, heterogeneous enhancement of the lesion 1d: In the ADC map, high ADC values with no restricted diffusion.

Statistical Analysis

The data were analyzed using SPSS software (version 22.0; IBM Corp., Armonk, NY). General linear model was used to analyze the power value of the univariate variables. Power values were between 0.812 and 0.879. The Mann–Whitney U test was used to compare the T1, T2, post-contrast SI, and ADC values between the malignant and benign lesions. The SI and ADC values for the most common two lesions (i.e., Warthin tumors and pleomorphic adenomas) were also compared using the Mann-Whitney U test. Spearman's correlation coefficient (ρ) was used to evaluate the association between non-parametric variables. The Pearson correlation coefficients (r) were calculated to determine relationships with respect to size, localization, contrast enhancement pattern, characteristics of surgical margins, perineural invasion, extension to adjacent structures, and lymph node involvement between malignant and benign lesions. A rho (r) value of 1 indicated a perfect positive correlation, while if $r = -1$, a perfect negative correlation was indicated. The quantitative variables were expressed as means, medians, standard deviations, and interquartile ranges, and the qualitative variables were expressed as frequencies or ratios. P-values <0.05 were considered statistically significant.

RESULTS

In total, 64 parotid gland lesions were evaluated. Two infantile parotid hemangiomas, one hemorrhagic cyst, one abscess, one case of sialadenitis, one

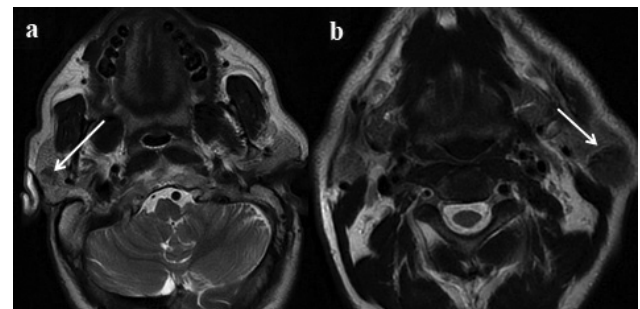


Figure 2a. Right-sided well-defined, 2b. Left-sided well-defined hypointense lesions in T2W axial images; bilateral Warthin tumors (arrows).

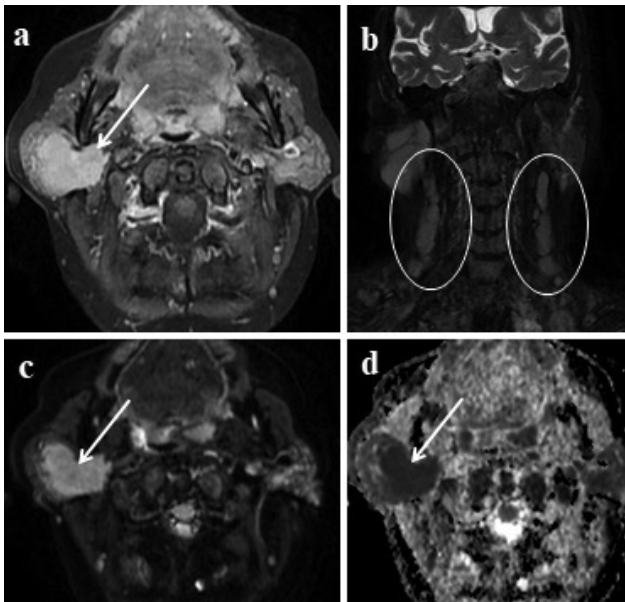


Figure 3. Lymphoma involvement of the parotid gland 3a: In contrast enhanced axial image; right-sided well-defined enhancing lesion involving almost the entire parotid gland is seen (arrow). **3b:** Multiple spheric and oval-shaped lymphadenopathies in the cervical region (circles) **3c, d:** Lesion shows marked diffusion restriction (arrows).

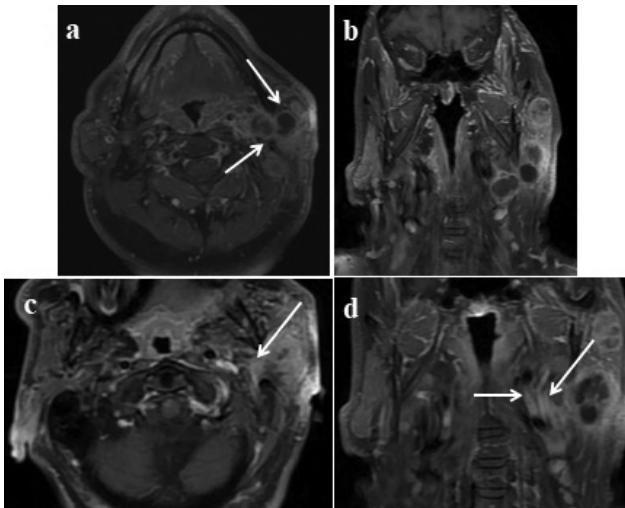


Figure 4. Multiple lesions in the deep and superficial lobes of the left parotid gland; proven mucoepidermoid carcinoma: Axial 4a: Post-contrast coronal T1W images show left-sided lesions with cystic necrotic areas, heterogenous contrast enhancement in the lesions involving deep and superficial lobes (arrows). 4c: Axial, 4d: T1W post-contrast coronal images; enhancement in the retromolar trigone is adjusted because of perineural spread (arrows).

cyst, and four lesions with image quality that was inadequate for evaluation were excluded from the study. After exclusion, the study included 42 patients (24 females, 18 males; mean age, 51.4±15.9 years)

with 54 parotid gland lesions. The size of the lesions ranged from 7 mm to 61 mm. The distribution of the lesions were as follows: pleomorphic adenomas (n=21), Warthin tumors (n=18) (Figure 2), lymph nodes (n=2), mucoepidermoid carcinomas (n=3) (Figure 3), adenoid cystic carcinomas (n=5), basal cell carcinoma, (n=1), metastatic lesions (squamous cell carcinoma) (n=2), and two lymphomas (Table 1). There were multiple lesions in nine patients.

Table 1. Distribution, location and characteristics of lesions.

| | n; | number percentage (%) |
|------------------------------|----|-----------------------|
| Diagnosis | | |
| Pleomorphic adenoma | 21 | 38.9 |
| Whartin tumor | 18 | 33.3 |
| Lymph node | 2 | 3.7 |
| Adenoid cystic carcinoma | 5 | 9.3 |
| Mucoepidermoid carcinoma | 3 | 5.5 |
| Lymphoma | 2 | 3.7 |
| Basalcellcarcinoma | 1 | 1.9 |
| Metastasis | 2 | 3.7 |
| Side | | |
| Right | 33 | 61.1 |
| Left | 21 | 38.9 |
| Marginfeature | | |
| Well defined | 32 | 59.3 |
| Lobulated | 10 | 18.5 |
| Ill defined | 12 | 22.2 |
| Localization | | |
| Superficial lobe | 30 | 55.6 |
| Deep lobe | 7 | 13.0 |
| Superficial and deep lobe | 17 | 31.5 |
| Extension | | |
| Exist | 9 | 16.7 |
| None | 45 | 83.3 |
| Perineural spread | | |
| Exist | 4 | 7.4 |
| None | 50 | 92.6 |
| Lymphadenopathy | | |
| Exist | 6 | 11.1 |
| None | 48 | 88.9 |
| Contrast enhancement pattern | | |
| Heterogenous | 27 | 50.0 |
| Homogenous | 20 | 37.0 |
| Peripheral | 5 | 9.3 |
| None | 2 | 3.7 |
| Character | | |
| Benign | 41 | 75.9 |
| Malignant | 13 | 24.1 |
| Size | | |
| <1 cm | 2 | 3.7 |
| 1-2 cm | 24 | 44.4 |
| 2-3 cm | 19 | 35.2 |
| >3 cm | 9 | 16.7 |

Table 2. Correlation of parametric data with each other.

| | Character | Gender | Size | Side | Localization | Margin features | Extansion | Perineural spread | Lymph-adenopathy | Enhancement pattern |
|------------------------|-----------|--------|---------|-------|--------------|-----------------|-----------|-------------------|------------------|---------------------|
| Character(r) | 1 | -,032 | ,140 | ,084 | ,247 | ,622** | -,678** | -,502** | -,490** | -,146 |
| Gender(r) | -,032 | 1 | -,283 | ,149 | -,323* | -,227 | -,059 | -,133 | ,053 | -,010 |
| Size(r) | ,140 | -,283 | 1 | ,066 | ,604** | ,253 | -,322* | -,036 | -,452** | -,185 |
| Side(r) | ,084 | ,149 | ,066 | 1 | -,040 | ,128 | -,153 | -,064 | -,201 | -,048 |
| Localization(r) | ,247 | -,323* | ,604** | -,040 | 1 | ,354** | -,340* | -,232 | -,291* | ,095 |
| Margin features(r) | ,622** | -,227 | ,253 | ,128 | ,354** | 1 | -,624** | -,471** | -,445** | -,104 |
| Extansion(r) | -,678** | -,059 | -,322* | -,153 | -,340* | -,624** | 1 | ,443** | ,632** | ,000 |
| Perineural spread(r) | -,502** | -,133 | -,036 | -,064 | -,232 | -,471** | ,443** | 1 | ,125 | ,238 |
| Lymphadenopathy(r) | -,490** | ,053 | -,452** | -,201 | -,291* | -,445** | ,632** | ,125 | 1 | ,000 |
| Enhancement pattern(r) | -,146 | -,010 | -,185 | -,048 | ,095 | -,104 | ,000 | ,238 | ,000 | 1 |

Character; malignant-benign, **Correlation Significant at $p < 0.01$ level, *Correlation Significant at $p < 0.05$ level, r; Pearson Correlation coefficient.

Table 3. Signal intensity and ADC values of benign and malignant lesions.

| | Benign (n=41) | Malignant (n=13) | p |
|---------------------------------------|------------------------|------------------------|--------|
| T1SI median (min-max), IQR | 666 (186-1383) 1197 | 576 (265-951) 332 | 0.154 |
| T2SI median (min-max), IQR | 738 (118-1871) 614 | 603 (511-958) 153 | 0.498 |
| Postkontrast SI median (min-max), IQR | 1260 (429-2924) 618 | 1218 (678-2127) 296 | 0.960 |
| ADC median (min-max), IQR | 1394 (536-2298) 890 | 776 (516-1533) 450 | 0.003* |

Mann Whitney U Test, IQR: Inter quartile range, min: minimum, max: maximum, ADC: apparent diffusion coefficient, SI: Signal intensity, T1SI: Signal intensity in T1 weighted sequence, T2SI: Signal intensity in T2 weighted sequence

However, all these lesions were either malignant or benign. Synchronous benign and malignant lesions were not detected in any of the cases. Forty-one (77.7%) benign and 13 (22.2%) malignant lesions were detected. No correlation was detected between the malignant and benign lesions based on demographic characteristics, size, laterality, or localization of the lesion ($r=0.032$, 0.140 , 0.084 , and 0.247 , respectively) (Table 2). The contrast enhancement pattern, pre- and post-contrast T1 SI

Table 4. Correlation analysis of non-parametric data with each other.

| | Character | T1SI | T2SI | SI C+ | ADC |
|----------------------|-----------|--------|--------|--------|---------|
| Character (ρ) | 1,000 | -,196 | -,093 | ,007 | -,413** |
| T1SI (ρ) | -,112 | 1,000 | ,443** | ,513** | ,038 |
| T2SI (ρ) | -,277* | ,443** | 1,000 | ,403** | ,491** |
| SI C+ (ρ) | -,172 | ,513** | ,403** | 1,000 | ,077 |
| ADC (ρ) | -,676** | ,038 | ,491** | ,077 | 1,000 |

Character: malign-benign, T1SI: Signal intensity in T1 weighted sequence, T2SI: Signal intensity in T2 weighted sequence, SI C+: Signal intensity after contrast injection, ADC: Apparent diffusion coefficient, **: Correlation Significant at $p < 0.01$ level, ρ : Spearman's correlation coefficient

also did not differ ($r=0.146$, $p=0.112$, and 0.172 , respectively) (Table 3). Morphologic parameters such as ill-defined margins, perineural spread, the presence of lymphadenopathy, and extension into adjacent structures were found to be significantly associated with malignant lesions ($p < 0.01$) (Table 2). There was a significant difference in the ADC values between the malign and benign lesions ($p < 0.05$) (Tables 3 and 4), and there were significant differences in the ADC values $p < 0.001$ and T2 SI ($p < 0.05$) between the Warthin tumors and pleomorphic adenomas. The ADC cut-off value for differentiation of the malignant and benign parotid tumors was calculated using the receiver operating characteristic (ROC) curve and was found to be 1.044×10^{-3} mm²/sec. Lesions above this value tended to be benign. At this cut-off value, the positive, and negative predictive values of ADC were 37.5% and 86.7%, respectively. Besides, the sensitivity, and

specificity of the test based on a cut-off value of ADC 1.044×10^{-3} were 69.2% and 86.7%, respectively. In the differentiation of pleomorphic adenoma and Warthin tumor, the cut-off value of T2 SI was 715. Lesions with lower SI were more likely to be a Warthin tumor. At this cut-off value of T2 SI, the sensitivity, specificity, positive and negative predictive values of the test were 61.9%, 66.7%, 68.4% and 60.0%, respectively.

DISCUSSION

In this study, we evaluated the effectiveness of morphological features, SI characteristics, and mean ADC values to differentiate malignant parotid gland lesions from benign parotid gland tumors. Our results revealed that ill-defined borders, extension into adjacent structures, perineural invasion, and lymph node involvement were associated with malign lesions. In contrast to the benign lesions, the ADC values were negatively correlated with the malignant lesions, and unlike the pleomorphic adenomas, they were negatively correlated with the Warthin tumors. The T2 SI values of the Warthin tumors were found to be lower than those of the pleomorphic adenomas.

It was stated that a sharp (well-defined) contour is an important feature supporting benignity⁹⁻¹², but some malignant tumors have this feature and can thus mimic benign tumors¹³. In line with previous studies, our results support the finding that well-defined contour margins of a tumor in the parotid gland may be a feature of benignity. An extension to the adjacent tissue and perineural invasion was also found to be significantly associated with malignant tumors. Although deep lobe involvement was reported as a feature of malignant tumors, inflammatory conditions and benign tumors such as Warthin tumors can also involve the deep lobe¹⁰. We could not find any significant association between malignant and benign lesions in terms of deep or superficial lobe localization. It was previously reported that the

tumor heterogeneity and T2 hypointensity may indicate malignancy, and it is not sufficient for precise differentiation⁸. Our results revealed that the T2 SI of the Warthin tumors was significantly lower than that of the pleomorphic adenomas. This may be attributed to the high cellularity and densely packed lymphoid tissue in Warthin tumors described in previous studies¹⁴⁻¹⁷.

According to the diffusion theory, ADC values are expected to decrease due to restricted diffusion in hypercellular tumors that contain densely packed cells¹⁸. In previous DWI studies, significant differences in ADC values were reported between benign and malignant head and neck tumors, including salivary gland tumors¹⁸. Also, it was reported that T2 SI is lower in Whartin tumors and malignant parotid tumors⁸. The morphological features of PGTs can be evaluated by MRI, but detecting the lesions and defining the features may not be sufficient to avoid a biopsy. FNAB is the most widely used biopsy technique for these lesions. A further goal of our study was therefore to evaluate whether ADC and T2 SI values may be an alternative to biopsy or at least reduce the number of biopsies performed. As previously indicated, the results of our study revealed that the ADC values were significantly lower for the malignant lesions, which implies that ADC values may be a useful tool for distinguishing between malignant and benign parotid gland lesions. Some DWI studies suggested that malignant PGTs were different from benign PGTs as they have lower ADC values. In a recent multiparametric MRI study, higher diagnostic accuracy of ADC values in differentiating pleomorphic adenomas from malignancies was demonstrated and ADC values were found to be also useful in differentiating Warthin tumors from malignant tumors¹⁴. We found lower ADC values in the malignant and Warthin tumors in our study and the ADC values provided diagnostic accuracy in the differentiation between malignant and benign tumors. Furthermore, the ADC values differed for the pleomorphic adenomas and the Warthin

tumors in our study. Since the clinical course and treatment of pleomorphic adenomas and Warthin tumors are different, it is remarkable that this distinction can be achieved without the need for a biopsy. This finding should therefore be supported by new studies.

Advanced MRI techniques such as functional and multiparametric MRI offer valuable information about the vascularity, structure, metabolite concentrations, cellularity, and behavioral course of tumors^{14,16,19-21}. Multiparametric MRI in the differentiation of PGTs is a current topic in head and neck radiology. Yabuuchi et al.¹⁵ analyzed the time SI curve (TIC) derived from dynamic contrast enhanced (DCE) MRI. The authors found that the washout ratio and time to peak were closely correlated with the cellularity grade and microvessel count of tumors¹⁶. A further study evaluated the diagnostic accuracy of multiparametric MRI in the differentiation of parotid gland tumors and similar results were found to those of Yabuuchi et al.¹⁵. According to Elmokadem et al.¹⁴ high sensitivity and specificity in the combined assessment of TIC types and washout rates were beneficial not only in differentiating between benign and malignant parotid tumors, but also in distinguishing Warthin tumors from others. The possibility of identifying the histopathologic types of tumors without biopsy may prevent unnecessary surgical interventions, decrease hospitalization time, and ease the treatment. Despite these developments in the use of dynamic examination and other parameters, it is difficult to use them in daily practice, particularly because of the duration of imaging. Given that many parotid lesions are detected incidentally, the importance of conventional MRI findings increases when dynamic MRI cannot be applied.

The small sample size of malignant tumors and their subtypes and the absence of DCE MRI were among limitations of our study. We aimed to counter these limitations by applying the recommended parameters as alternatives to

dynamic MRI examination. Further studies with larger sample sizes and different subtypes would improve future findings.

Conventional MRI and DWI may guide the diagnosis in cases where the use of contrast agents should be avoided, such as in patients with renal dysfunction and where imaging quality is expected to be inadequate for dynamic imaging due to long exposure times.

CONCLUSION

We suggest measuring T2 SI and ADC values in addition to morphological evaluation. Thus, malignant tumors can be distinguished from benign lesions and Warthin tumors from pleomorphic adenomas, and the number of biopsies therefore its complications can be reduced.

REFERENCES

1. Pinkston JA, Cole P. Incidence rates of salivary gland tumors: results from a population-based study. *Otolaryngol Head Neck Surg.* 1999;120:834-40. [CrossRef]
2. Magnano M, Gervasio CF, Cravero L, et al. Treatment of malignant neoplasms of the parotid gland. *Otolaryngol Head Neck Surg.* 1999;121:627-32. [CrossRef]
3. Gökçe E. Multiparametric magnetic resonance imaging for the diagnosis and differential diagnosis of parotid gland tumors. *J Magn Reson Imaging.* 2020;52:11-32. [CrossRef]
4. Freling N, Crippa F, Maroldi R. Staging and follow-up of high-grade malignant salivary gland tumours: The role of traditional versus functional imaging approaches - a review. *Oral Oncol.* 2016;60:157-66. [CrossRef]
5. Speight PM, Barrett AW. Salivary gland tumours. *Oral Dis.* 2002;8:229-40. [CrossRef]
6. Yousem DM, Kraut MA, Chalian AA. Major salivary gland imaging. *Radiology.* 2000;216:19-29. [CrossRef]
7. Abdel Razek AA, Samir S, Ashmalla GA. Characterization of parotid tumors with dynamic susceptibility contrast perfusion-weighted magnetic resonance imaging and diffusion-weighted MR imaging. *J Comput Assist Tomogr.* 2017;41:131-6. [CrossRef]
8. Karaman CZ, Tanyeri A, Özgür R, Öztürk VS. Parotid gland tumors: comparison of conventional and diffusion-weighted MRI findings with histopathological results. *Dentomaxillofac Radiol.* 2021;50:420200391. [CrossRef]
9. Christe A, Waldherr C, Hallett R, Zbaeren P, Thoeny H. MR imaging of parotid tumors: typical lesion characteristics in MR imaging improve discrimination between benign and malignant disease. *AJNR Am J Neuroradiol.* 2011;32:1202-7. [CrossRef]
10. Ikeda M, Motoori K, Hanazawa T, et al. Warthin tumor

- of the parotid gland: diagnostic value of MR imaging with histopathologic correlation. *AJNR Am J Neuroradiol.* 2004;25:1256-62. PMID: 15313720
11. Xu ZF, Yong F, Yu T, et al. Different histological subtypes of parotid gland tumors: CT findings and diagnostic strategy. *World J Radiol.* 2013;5:313-20. [CrossRef]
 12. Choi DS, Na DG, Byun HS, et al. Salivary gland tumors: evaluation with two-phase helical CT. *Radiology.* 2000;214:231-6. [CrossRef]
 13. Eida S, Sumi M, Nakamura T. Multiparametric magnetic resonance imaging for the differentiation between benign and malignant salivary gland tumors. *J Magn Reson Imaging.* 2010;31:673-9. [CrossRef]
 14. Elmokadem AH, Abdel Khalek AM, Abdel Wahab RM, et al. Diagnostic accuracy of multiparametric magnetic resonance imaging for differentiation between parotid neoplasms. *Can Assoc Radiol J.* 2019;70:264-72. [CrossRef]
 15. Yabuuchi H, Fukuya T, Tajima T, Hachitanda Y, Tomita K, Koga M. Salivary gland tumors: diagnostic value of gadolinium-enhanced dynamic MR imaging with histopathologic correlation. *Radiology.* 2003;226:345-54. [CrossRef]
 16. Yabuuchi H, Matsuo Y, Kamitani T, et al. Parotid gland tumors: Can addition of diffusion-weighted MR imaging to dynamic contrast-enhanced MR imaging improve diagnostic accuracy in characterization? *Radiology.* 2008;249:909-16. [CrossRef]
 17. Aghaghazvini L, Salahshour F, Yazdani N, et al. Dynamic contrast-enhanced MRI for differentiation of major salivary glands neoplasms, a 3-T MRI study. *Dentomaxillofac Radiol.* 2015;44:20140166. [CrossRef]
 18. Thoeny HC, De Keyzer F, King AD. Diffusion-weighted MR imaging in the head and neck. *Radiology.* 2012;263:19-32. [CrossRef]
 19. Takashima S, Noguchi Y, Okumura T, Aruga H, Kobayashi T. Dynamic MR imaging in the head and neck. *Radiology.* 1993;189:81. [CrossRef]
 20. Salama AA, El-Barbary AH, Mlees MA, Esheba GE-S. Value of apparent diffusion coefficient and magnetic resonance spectroscopy in the identification of various pathological subtypes of parotid gland tumors. *Egypt J Radiol Nucl Med.* 2015;46:45-52. [CrossRef]
 21. Abdel Razek AA, Poptani H. MR spectroscopy of head and neck cancer. *Eur J Radiol.* 2013;82:982-9. [CrossRef]